Astron. Astrophys. 326, 851–859 (1997)

ASTRONOMY
AND
ASTROPHYSICS

Dynamics of the solar granulation

IV. Granular shear flow

A. Nesis[1], **R. Hammer**[1], **A. Hanslmeier**[2], **H. Schleicher**[1], **M. Sigwarth**[1], **and J. Staiger**[1]

[1] Kiepenheuer-Institut für Sonnenphysik, Schöneckstr. 6, D-79104 Freiburg, Germany (Internet: nesis@kis.uni-freiburg.de)
[2] Institut für Astronomie, Universitätsplatz 5, A-8010 Graz, Austria

Received 11 February 1997 / Accepted 23 April 1997

Abstract. Strong velocity gradients at granular borders appear to be the source of unresolved velocity fluctuations detectable as line broadening variations of magnetically and thermally insensitive absorption lines. Based on spectrograms of high spatial and spectral resolution taken with the German Vacuum Tower Telescope (VTT) in Izaña (Tenerife) we study the strong velocity gradients and the unresolved velocity field as well as their mutual interaction. We also investigate the variation of these quantities with the height in the photosphere, for both a regular and an exploding granule. By means of a coherence analysis we study, furthermore, the extension of the convective and turbulent fluctuation field of the granulation layers into the overlying overshoot layers as a function of the wavenumber. The results of the coherence analysis are consistent with, and complementary to, those obtained from the investigation of regular and exploding granules.

The small and large scales of the convective and unresolved velocity field behave clearly different as far as their penetration into the overlying photospheric layers is concerned. One pressure scale height above the continuum we find an unresolved velocity field that does not show any resemblance to the same velocity field at the continuum level. We find that the symmetry behavior of the unresolved velocity field with respect to the granular flow varies with the height in the photosphere.

The unresolved velocity field could be of oscillatory, convective, or turbulent character. However, the fact that the unresolved velocity field is more prominent at the granular border, which is also the location of strong shear flow, favors its turbulent character. In this sense the granules can be seen as quasi-laminar convective flows emerging in the turbulent field of the overshoot layers.

Key words: Sun: photosphere – Sun: granulation

Send offprint requests to: A.Nesis

1. Introduction

The dynamical state of the granulation is characterized by strong velocity gradients located at the granular borders immediately adjacent to the intergranular space.

First observational indications of strong velocity gradients at the granular borders came from spectrograms of high spatial and spectral resolution taken at the center of the solar disk with the VTT in Izaña (Tenerife, Spain) (cf. Nesis et al. 1992). These spectrograms also showed enhanced turbulence located in the intergranular space and especially at the granular borders, associated with strong vertical gradients (Nesis et al. 1993). New observations taken in 1994 provided further evidence of shear flow and turbulent spots at the granular borders (Nesis et al. 1996a,b).

The importance of the shear flow for the understanding of the dynamics of the photosphere and the physics of the granulation is obvious. According to some recent investigations, other physical processes, like global oscillations (Christensen-Dalsgaard 1996) and granular fragmentation (Rast 1995), depend sensitively on the dynamical state of the granulation layers and, thus, on the turbulent shear in the overshoot layers. Brown (1991) asserted "that the source exciting the solar p-modes is likely to be acoustic noise generated in the top part of the Sun's convection zone" and argued that "if so, then simple arguments suggest that most of the emitted energy may come from rare localized events that are well separated from one another in space and time". Rimmele et al. (1995) located "acoustic events" in the photosphere, preferentially in the intergranular space, the place of enhanced turbulence; and Espagnet et al. (1995) found the intergranular space, especially the place with strong downwards velocities, to be the origin of the acoustic oscillations in the photosphere, which gives indirect evidence for the activity of turbulent shear. In their recent work Ghosh et al. (1995) show that velocity profile and depth of the shearing velocity field of the upper convective layers are important for the understanding of the discrepancy between observations and current theoretical interpretations of the f-mode frequency of the solar global oscillations. Horizontal granular velocities and their gradients

with the height can only be recognized in the case of solar limb observations. Nesis et al. (1990), using spectrograms taken at the solar limb with the balloon-borne *Spektrostratoskop*, found a rapid variation of the horizontal granular velocity with height in the photosphere and inferred the existence of boundary layers just above the granules, indicative of vertical shear flow. Heming (1989) asserted the existence of velocity vortices in the granulation layers associated with strong gradients of the horizontal granular velocity.

We believe therefore that an investigation of the turbulent shear flows at the granular borders is important and can be approached best by studying the properties of both the turbulent velocity field and the strong velocity gradients as well as their mutual interaction. This type of study must consider the evolution of granules with height.

Thus the principal aim of this paper is to investigate the similarity between the turbulence fields at different heights in the photosphere. We do that using lines of zero or small Landé factors, which are formed at different heights. The observed region is magnetically nonactive. By means of power and coherence analyses we investigate the relationship between the velocity fields at different heights. The velocity gradients are investigated on the basis of two characteristic types of granules: a regular granule with the maximum of its flow in its center, and an exploding granule with maxima of the flow at its borders.

In this investigation we address mainly the turbulence: its height dependence, its generation, and its relationship to the granular velocity. Furthermore, we are interested in the granular velocity patterns and their height variation. We hope that this investigation provides some insight into the physics of the origin of the turbulence in the deep photosphere.

2. Material and method

2.1. Material

The material on which this study is based consists of photographic spectrograms taken with the German Vacuum Tower Telescope (VTT) in Izaña (Tenerife) in May 1994. A series of spectrograms was taken at the same position on the solar disk every 15 sec, covering about 5 min in total. The exposure time was 4 sec. The wavelength range was $\lambda\lambda$: 491.00 — 491.40 nm, the slit width 60 μ.

Fig. 1 shows part of our best spectrogram. It was selected from the series by judging the spatial resolution both visually (in terms of the detail in the line wiggles as seen in a microscope) and numerically (from the properties of the power spectra, which are discussed below). It shows fine structure and power above the noise level down to the intrinsic resolution limit of the instruments, so that atmospheric seeing effects should be negligible. The results shown in the following figures refer to this best spectrogram, although we have confirmed them with a number of other spectrograms of slightly lower quality. Since all other spectrograms are of lower quality, we have not used them to derive quantitative statistical properties such as mean values and standard deviations for our results.

The spectrograms were digitized with the microphotometer of the Kiepenheuer-Institut at steps of 30μ in the direction of dispersion (which corresponds to 0.26×10^{-3} nm). Perpendicular to the direction of dispersion the step width was also 30 μ (corresponding to 0.138 arcsec). The aperture size of the microphotometer was the same as the step width (30 $\mu \times 30\ \mu$).

In this work we used the lines Fe Ip 491.15 nm, Fe I 491.18 nm, Ni I 491.20 nm, Fe I 491.25 nm and the unidentified line 491.31 nm. The first two lines have Landé factors g=1.25 and 1.50, respectively, the Ni I line is magnetically insensitive with g=0.00. The line Fe I 491.25 nm has a Landé factor of g=1.04, whereas for the unidentified line we miss any data. Line profiles were computed under LTE assumption for the photospheric model of Holweger & Müller (1974). Oscillator strengths and correction factors for van de Waals damping were adjusted such that the computed profiles gave a satisfactory match to the Kitt Peak FTS Spectral Atlas. Contribution functions of the line depression were calculated according to Eq. 21 of Magain (1986). The maximum of the contribution function at line center was taken as "formation height" of a line. The line centers of Fe I 491.18 nm and Ni I 491.20 nm are formed at a height of approximately 200 km above the continuum at $\tau_{5000} = 1$. The lines FeIp 491.15 nm and FeI 491.25 nm are formed deeper, at heights of 130 km and 100 km, respectively. The observed line strength fluctuation of the unidentified line at 491.31 nm is quite small indicating that its temperature sensitivity is weak, like high excitation lines of neutral metals or low excitation lines of singly ionized metals. For both cases we find formation heights of about 70 km for a line with the observed equivalent width. All heights are relative to the continuum level at $\tau_{5000} = 1$.

2.2. Method

With these absorption lines we could measure Doppler velocity as well as line broadening fluctuations *simultaneously* at different heights in the photosphere within the first 200 km above the continuum. Both the Doppler velocity fluctuations v and the line broadening fluctuations FWHM were measured along the spectrograph slit s at all scanned positions s_i ($i = 0, 1, \cdots, 676$); the v variations are measured as Doppler shift fluctuations of the line core while the line broadening fluctuations FWHM correspond to the full line width at half maximum (cf. Nesis et al. 1993). Because the absorption lines are to first order magnetically and thermally insensitive and the line asymmetry is negligible, FWHM reflects, thus, an unresolved photospheric velocity field which unambiguously includes photospheric turbulent velocity fluctuations w. Calculating the line profiles we verify that the lines have a small temperature sensitivity, as expected for neutral metal lines of ca. 4 eV excitation.

To keep track of the granular dynamics, i.e. of the turbulent and the granular velocity field, as well as of the turbulent and the granular velocity pattern at various photospheric layers within the first 200 km above the continuum, we proceed in two steps: (i) We study the convective and turbulent flow in the layers overlying two characteristic types of granules: an exploding and

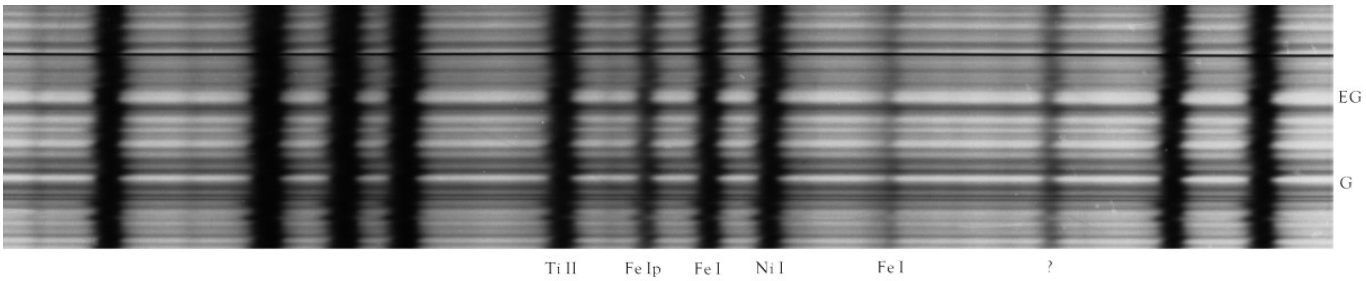

Fig. 1. Part of our best spectrogram showing two characteristic types of granules: a regular (G) and an exploding (EG) one, separated by 15 arcsec. The lines used in this study are identified; their wavelengths and formation heights are given in Sect. 2.1.

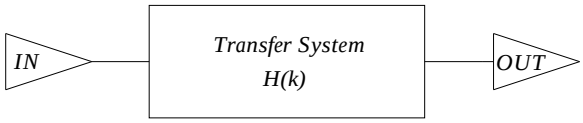

Fig. 2. Ideal single-input/single-output transfer system.

a regular one: We compare the traces of the Doppler velocity and turbulent velocity fluctuations as a function of height in the photosphere above the two granules; and the symmetry of the location of the enhanced turbulence with respect to the granules at the various photospheric layers.
(ii) We investigate the dynamical behavior of the turbulent and the granular velocity pattern with height in the photospheric layers by means of the coherence analysis.

The first step is very useful for a detailed discussion of the dynamical behavior concerning the convective and turbulent flow over single granules, especially in the case of morphologically different granules probed by our set of spectral lines. The second step concerns all the spatial patterns which synthesize the convective and turbulent field and moreover operate with mean values, thus complementing the first step.The second step is described briefly in the following two paragraphs.

Coherence analysis: basic considerations.- The coherence analysis is defined here for a one-dimensional single-input/single-output *transfer system* (cf. Fig. 2). The input $x(s)$ and output $y(s)$ are real-valued functions of the space coordinate s. The frequency response function $H(k)$ is system specific and depends on the wavenumber k.

Assuming that the power functions $P_{xx}(k)$ and $P_{yy}(k)$ are both different from zero, the *coherence function* between the input $x(s)$ and the output $y(s)$ is a real-valued quantity defined by

$$\gamma^2_{xy}(k) = \frac{|P_{xy}(k)|^2}{P_{xx}(k)P_{yy}(k)},$$

where $P_{xy}(k)$ is the *input/output cross-power*. The coherence function satisfies $0 \leq \gamma^2_{xy}(k) \leq 1$.

In the ideal case of a perfect *transfer system* the coherence function will be unity; in this case $x(s)$ and $y(s)$ are completely dependent. The case $\gamma^2_{xy}(k) = 0$ means that $x(s)$ and $y(s)$ are completely independent. If the coherence function is greater than zero but less than unity, the system relating $x(s)$ and $y(s)$ could be nonlinear, or extraneous noise could be present in the measurements.

The *absolute value* and *phase angle* are determined by

$$|P_{xy}(k)| = \sqrt{C^2_{xy}(k) + Q^2_{xy}(k)}$$

$$\theta_{xy}(k) = \tan^{-1}\frac{Q_{xy}(k)}{C_{xy}(k)}.$$

where $Q_{xy}(k)$ is the quadrature spectral density function (one-sided), and $C_{xy}(k)$ is the coincident spectral density function (one-sided).

Coherence analysis: application to the investigation of photospheric velocity fields.- We applied the coherence analysis to investigate the dynamical properties of photospheric layers, especially the response of these layers to the turbulent and the Doppler velocity field of the granules. We proceeded as follows: assuming that the layer at 70 km above the continuum reflects the dynamics of the granulation, we considered it as the reference layer (input of the transfer system, Fig. 2) and calculated the coherence between this reference layer and the layers at 100, 130, 180/200, and 200 km (output of the transfer system Fig. 2), successively. Then we took the layer 130 km above $\tau_{5000} = 1$ as reference layer because it is approximately one pressure scale height above the continuum and reveals practically the minimum of the convective overshoot velocity. We applied thus the coherence analysis between the field at 130 km and those at 180/200 km and 200 km.

3. Results

3.1. Simultaneous observations of the turbulent and Doppler velocity field at various photospheric heights

Fig. 3 shows a snapshot of the Doppler velocity and turbulent fluctuations settled in the photospheric layers over two characteristic granules. Specifically, the right column exhibits the dynamical state of the photospheric layers caused by the emergence of a regular granule, whereas the left column reveals the dynamical state of the same layers over an exploding granule. The panels *a, b, c, d,* and *e* show the convective flow and turbulent field at the heights 70, 100, 130, 180/200, and 200 km above

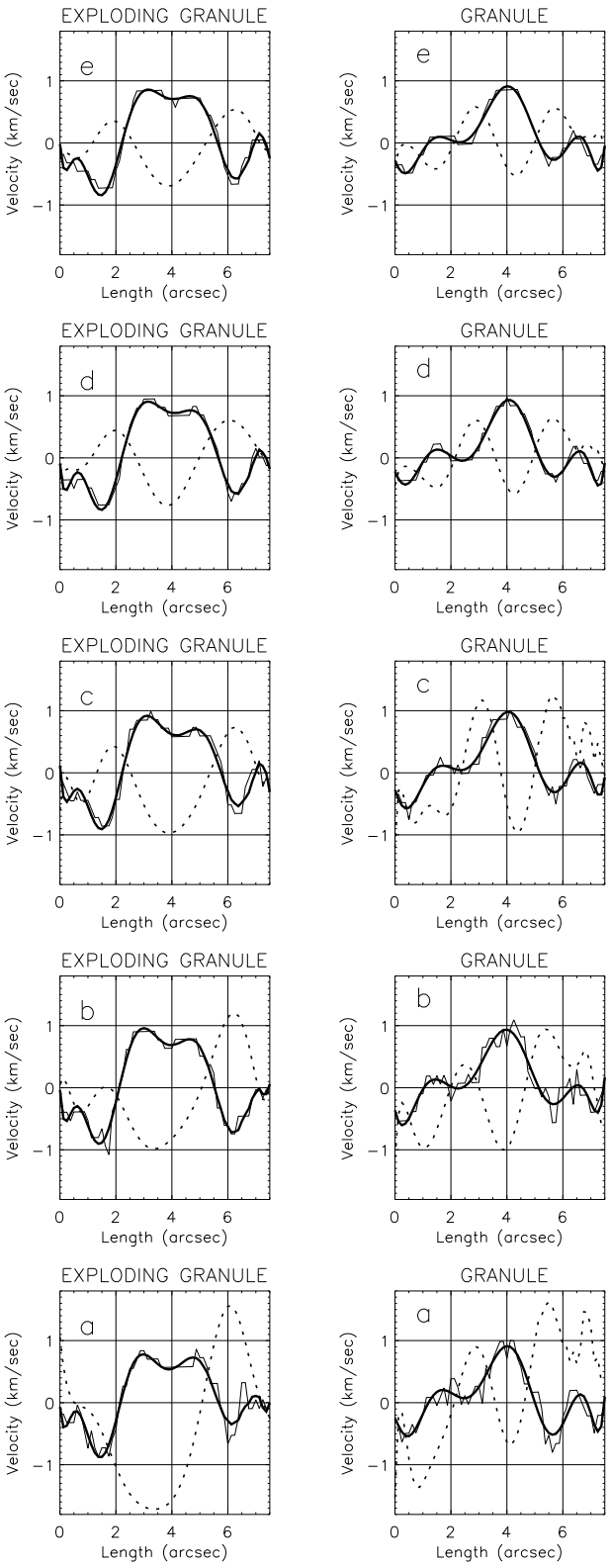

Fig. 3a–e. Simultaneous observations of the Doppler velocity v (thin solid line and heavy full line) and the turbulent velocity w (dotted line) of a normal granule (right column) and an exploding granule (left column) at the heights 70 km (panel *a*), 100 km (panel *b*), 130 km (panel *c*), 180/200 km (panel *d*), and 200 km (panel *e*) above $\tau_{5000} = 1$.

$\tau_{5000} = 1$, respectively. The *thin and heavy full lines* stand for the Doppler velocity v, measured and fitted by a ninth order polynomial, respectively. The velocity v is associated with the granular and intergranular convective flows, where positive and negative values mark upflow and downflow, respectively. The *dotted line* represents the turbulent velocity field w measured as line broadening. We subtracted the mean line width, so that positive and negative values of the line broadening fluctuations refer to enhanced or reduced turbulent field, respectively. It is noticeable that within the granules the line broadening is in practically all cases reduced, indicating a quasi-laminar flow.

Since the equivalent widths of these lines remain mostly constant along the slit, we tend to interpret the measured turbulence in terms of macroturbulence (cf. Traving 1964).

Regular granule.- Panels *a* to *e* in the right column illustrate the dynamical response of the photospheric layers overlying a normal granule. In detail we find the following:

(i) In the granule the upflow (heavy full line) has its maximum in the granular center with a velocity $\approx 800\,\mathrm{m\,sec^{-1}}$, which remains practically unchanged with the height in the photosphere. In the intergranular space, however, the downflow (heavy full line) seems to be stronger in the deepest layer (panel *a*) than in the layers above: At the right-hand side of the granule the Doppler velocity changes from approximately $-500\,\mathrm{m\,sec^{-1}}$ in panel *a* to approximately $-250\,\mathrm{m\,sec^{-1}}$ in all other panels.

(ii) In the granule the line broadening is *reduced* while in the intergranular space it is *enhanced*; but in both cases it changes significantly with height. Within the granules we find for this broadening -expressed in turbulent velocity (dotted line)- negative amplitudes exceeding $-500\,\mathrm{m\,sec^{-1}}$ in panels *a, b* and *c*; however, smaller values in panels *d* and *e*. In the intergranular space the amplitudes of the turbulent velocity fluctuations change from $\geq 1000\,\mathrm{m\,sec^{-1}}$ in panels *a, b,* and *c* to values $\leq 1000\,\mathrm{m\,sec^{-1}}$ in panels *d* and *e*.

(iii) In the intergranular space the turbulent velocity field is distributed asymmetrically with respect to the granular flow in the deep layers (panels *a* and *b*), but symmetrically at higher layers (panels *c, d,* and *e*). A large part of the observed velocity pattern is plausibly of convective origin. In addition, there might be an oscillatory contribution. Several authors have attempted in the past to separate both, with controversial results, as discussed by Espagnet et al. (1995). This subject will be also addressed in Sect. 4 below.

Exploding granule.- The left column of Fig. 3 shows:

(i) In the exploding granule the upflow (heavy full line) has a minimum in the granular center, and a maximum at the border. This changes with the height in the photosphere. In panel *a* the velocity difference between the borders and the center of the granule amounts to $\leq 300\,\mathrm{m\,sec^{-1}}$, but due to an increase of the velocity at one of the maxima the difference amounts to $\geq 300\,\mathrm{m\,sec^{-1}}$, in panels *b* and *c*. In panels *d* and *e* the minimum velocity increases and, thus, the difference decreases again. The

downflow (full heavy line) on both sides of the granular flow exhibits also a variation that decreases substantially with height. (ii) The behavior of the turbulent velocity field resembles that of the regular granule. We realize again large turbulent fluctuations *asymmetrically* located at the granular border in the deep layers (panels *a* and *b*), and moderate turbulent fluctuations *symmetrically* located at the granular border in panels *c, d* and *e*.

Although the above results allow us valuable insight into the dynamics of the photospheric layers above the granulation, they concern only two granules. We complement therefore our work with a statistical investigation of the entire data in the following part of this section.

3.2. Turbulence fluctuations

Coherence between granulation layers and the layers above.- In Fig. 4 the panels *a, b, c,* and *d* show the coherence functions $\gamma^2_{ww}(k)$ (left column) and the corresponding phase functions $\theta_{ww}(k)$ reflecting the relationship between the turbulence velocity fluctuations w of the deepest layers (70 km) above τ_{5000} = 1 and the turbulence velocity fluctuations of the higher photospheric layers, namely 100 km (panel *a*), 130 km (panel *b*), 180/200 km (panel *c*), and 200 km (panel *d*), respectively. In each panel the abscissa gives the wavenumber k in Mm^{-1}. At the top of each plot in the left column we have written spatial scales in arcsec. In order to follow the changes of the coherence behavior with height in the photosphere we ordered the panels in a column in increasing height. The coherence functions $\gamma^2_{ww}(k)$ in panels *a, b, c,* and *d* (left column) have the following noteworthy properties: (i) A high coherence within the range $0 \leq k \lesssim 5$. The values vary slightly with height in the photosphere from $\gamma^2_{ww} \approx 0.8$ in panel *a* to $\gamma^2_{ww} \approx 0.6$ in panel *d*; (ii) an abrupt decrease of the coherence value at $k \approx 5$ in all four panels; (iii) a small coherence within the range $7 \lesssim k \lesssim 17$, with $\gamma^2_{ww} \leq 0.25$, which appears to become even smaller with height in the photosphere.

Phase.- Panels *a, b, c,* and *d* of the right column in Fig. 4 show the phase function $\theta_{ww}(k)$ corresponding to the coherence function $\gamma^2_{ww}(k)$ in the left column. In panel *a* the phase θ_{ww} shows a moderate increase with wavenumber up to $k \approx 15$. For $k \gtrsim 15$ the variations of θ_{ww} are erratic. However, in panels *b, c,* and *d*, θ_{ww} changes to negative phase values compared to that in panel *a* for wavenumbers $k \lesssim 5$; θ_{ww} becomes irregular for $k \gtrsim 7$.

Coherence between middle layers (130 km) and the layers above.- In Fig. 5 panels *a* and *b* (left column) show the coherence functions $\gamma^2_{ww}(k)$ between the turbulence fluctuations of the middle photospheric layers (130 km above τ_{5000} = 1) and those of the higher layers at 180/200 km and 200 km. The axes of the plots in Fig. 5 correspond to those of Fig. 4. Panels *a* and *b* in Fig. 5 show (i) a high coherence in the range $0 \leq k \lesssim 7$, with $\gamma^2_{ww} \approx 0.8$, and (ii) a roughly linear decrease of the coherence as a function of k up to $k \approx 20$, where γ^2_{ww} changes from 0.7 at $k \approx 5$ to 0.3 at $k \approx 15$.

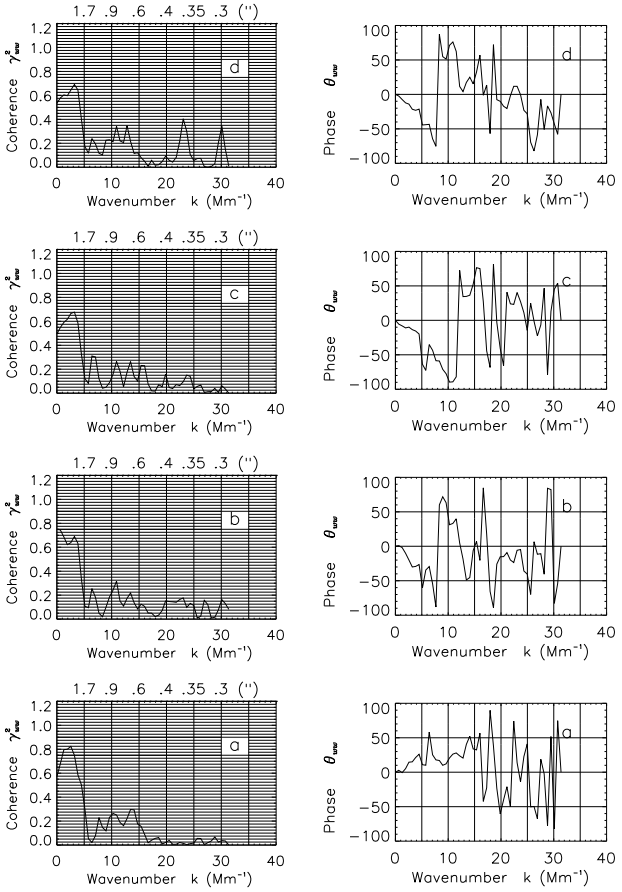

Fig. 4a–d. Coherence function $\gamma^2_{ww}(k)$ (left column) and the corresponding phase function $\theta_{ww}(k)$ (right column) between turbulent velocity fluctuations w at the layers 70 km above τ_{5000} = 1 and the turbulent fluctuations at various higher layers, namely 100 km (panel *a*), 130 km (panel *b*), 180/200 km (panel *c*), and 200 km (panel *d*), respectively, above τ_{5000} = 1.

Phase.- The right column of Fig. 5 shows the corresponding phase function $\theta_{ww}(k)$. In the range $0 \leq k \lesssim 7$ in panel *a* and $0 \leq k \lesssim 15$ in panel *b* the phase function remains close to zero; while in the range $7 \lesssim k \lesssim 15$ in panel *a*, θ_{ww} increases with k up to ≈50 deg. In both panels *a* and *b*, the $\theta_{ww}(k)$ function is erratic for wavenumbers higher than $k \approx 15$.

3.3. Doppler velocity fluctuations

Coherence between the granulation layers and the layers above.- In Fig. 6 panels *a, b, c,* and *d* in the left column show the coherence functions $\gamma^2_{vv}(k)$ between the velocity fluctuations v of the deepest (70 km above τ_{5000} = 1) and those at the higher photospheric layers, namely 100 km (panel *a*), 130 km (panel *b*), 180/200 km (panel *c*), and 200 km (panel *d*), respectively, above τ_{5000} = 1. In each panel the ordinate shows the coherence γ^2_{vv} whereas the abscissa gives the wavenumber k in Mm^{-1}. At the top of each plot we have indicated the spatial scale in arcsec corresponding to the wavenumber scale. The coherence functions in panels *a, b, c,* and *d* in Fig. 6 exhibit two clearly separated

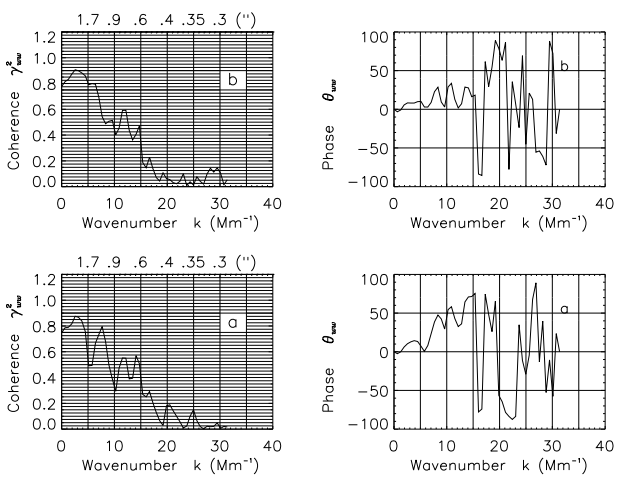

Fig. 5a and b. Coherence function $\gamma^2_{ww}(k)$ and the corresponding phase function $\theta_{ww}(k)$ between turbulent velocity fluctuations w at the layer 130 km above τ_{5000} = 1 and the turbulent fluctuations at the higher layers, namely 180/200 km (panel a), and 200 km (panel b), respectively, above τ_{5000} = 1.

ranges: (i) the range $0 \leq k \lesssim 5$, with $\gamma^2_{vv} \approx 0.9$; and (ii) the range $k \gtrsim 7$, where $\gamma^2_{vv} \approx 0.1$. Furthermore, we find that in all panels the coherence function drops to zero at the same wavenumber $k \approx 7$.

Phase.- Panels *a, b, c,* and *d* in the right column of Fig. 6 show the corresponding phase function $\theta_{vv}(k)$. We notice a similar behavior of the phase function $\theta_{vv}(k)$ in all panels: it remains constant, $\theta_{vv}(k) \approx 0$, up to $k \approx 7$ and begins to be erratic at $k \gtrsim 10$.

Coherence between the middle layers (100 km) and the layers above.- Panels *a* and *b* in Fig. 7 show the coherence functions $\gamma^2_{vv}(k)$ between the velocity fluctuations v of the middle photospheric layers (130 km) and those at 180/200 km and 200 km, respectively. The axes of the plots in Fig. 7 correspond to those of Fig. 5. The coherence functions are characterized by three ranges: (i) the range $0 \leq k \lesssim 5$, with $\gamma^2_{vv} \approx 0.9$; (ii) the range $5 \lesssim k \lesssim 10$, where γ^2_{vv} decreases practically linearly to values near zero and shows, thus, a moderate coherence; and (iii) the range $k \gtrsim 10$, with $\gamma^2_{vv} \approx 0.1$.

Phase The right column in Fig. 7 shows the corresponding phase function $\theta_{vv}(k)$. Here, $\theta_{vv}(k)$ reflects the behavior of the coherence function $\gamma^2_{vv}(k)$; it begins to become erratic for wavenumbers $k \geq 10$ and demonstrates thus the existence of small scale coherences in the higher layers.

4. Discussion

As shown in the right and left column of Fig. 3, the extension of the convective flow into the layers overlying the granulation can be easily followed for both regular and exploding granules.

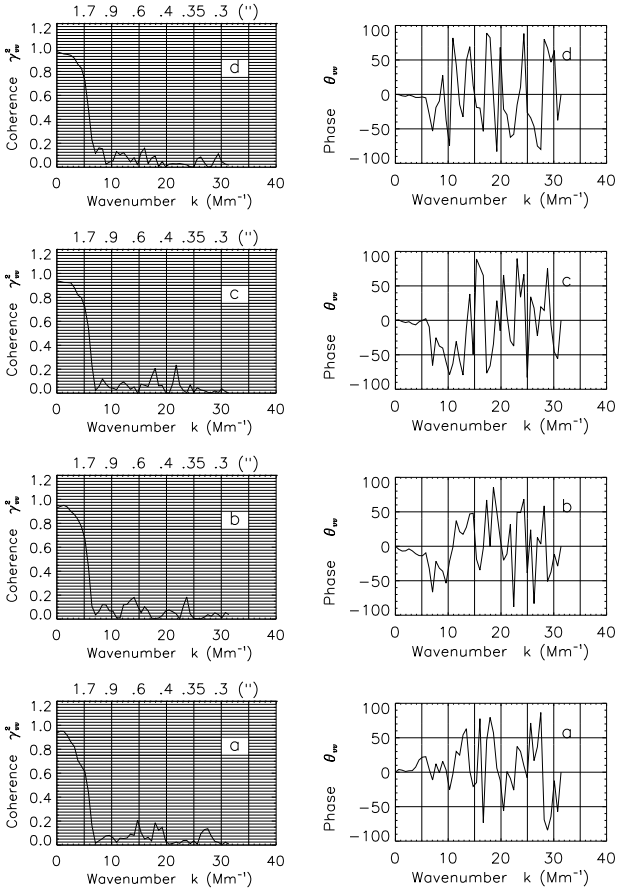

Fig. 6a–d. Coherence function $\gamma^2_{vv}(k)$ and the corresponding phase function $\theta_{vv}(k)$ between Doppler velocity v at the layer 70 km above τ_{5000} = 1 and the velocity at various higher layers, namely 100 km (panel *a*), 130 km (panel *b*), 180/200 km (panel *c*), and 200 km (panel *d*), respectively, above τ_{5000} = 1.

The relative constancy of the velocity profiles of the convective upflow and adjacent intergranular downflow of both types of granules manifests unambiguously the dominance of the overshoot flow of large granules throughout the photosphere up to $\approx$ 200 km above the continuum. A similar finding was reported recently by Strauss & Bonaccini (1997). Komm et al. (1990) reported a coherence decline for large structures beginning in the layers between 140 km and 190 km above τ_{5000} = 1, while Espagnet et al. (1995) report coherence throughout the entire photosphere.

Rast (1995), in his work on the nature of exploding granules and granule fragmentation, used as observational support for his theoretical argumentation our spectrogram. The similarity between the theoretical and observed velocity profiles of the exploding granule (see Fig. 3, left column, and Rast 1995, Fig. 4b) is remarkable.

The fact that the exploding and regular granule both show a constant convective velocity in the deep photosphere (heavy full line in Fig. 3, panels *a* — *b*) infers the lack of a significant velocity gradient with height, and implies that the granular flow *overshoots* into the convectively stable layers like a

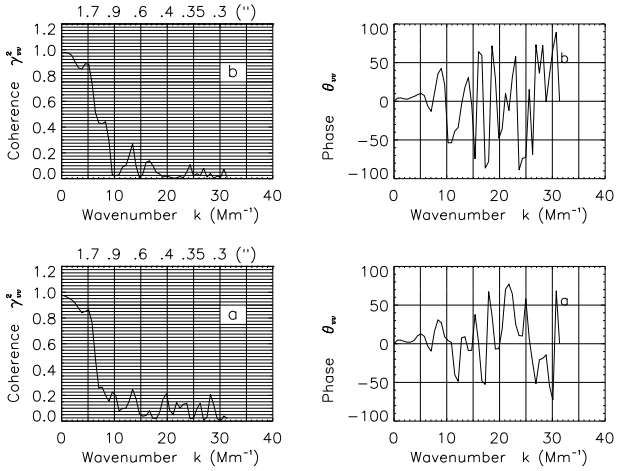

Fig. 7a and b. Coherence function $\gamma^2_{vv}(k)$ and the corresponding phase function $\theta_{vv}(k)$ between Doppler velocity fluctuations v at the layer 130 km above $\tau_{5000} = 1$ and the velocity fluctuations at the higher layers 180/200 km (panel *a*) and 200 km (panel *b*), respectively, above $\tau_{5000} = 1$.

quasi-laminar jet. We denote the jet as quasi-laminar because of the reduced turbulence (dotted line) found within the granules. Compared to this the shear flow at the granular border is much more turbulent.

The turbulent velocity field and its symmetry behavior with respect to the granular flow shows a distinct variation with height in the photosphere (cf. Figs. 3, left and right column, dotted line). For both the normal and exploding granule the noticeably asymmetrical form of the turbulent fluctuations within the first 100 km above the continuum (cf. Fig. 3 *a* and *b*) changes to a surprisingly symmetrical form in the overlying layers (panels *c* – *e*). It is remarkable that the symmetry behavior of the turbulent velocity field is the same for both types of granules in spite of their presumably different fragmentation mechanisms.

A turbulent velocity field in the intergranular space was also found by Altrock & Musman (1976). They investigated the physical conditions in the granulation by means of absorption lines and found evidence for the existence of turbulence (enhanced line broadening) in the intergranular space, which they assumed to be of Kolmogorov type. Nesis et al. (1993, 1996a) calculated the power spectrum of the turbulent velocity fluctuations w measured at the granulation layer and found that the spectral energy density of the turbulent field is given by a power-law k^{-2}, which is slightly steeper than the Kolmogorov power-law $k^{-5/3}$. We think it is satisfying that in these different investigations a turbulence field was found in the intergranular space.

What is the mechanism that could produce turbulence in the intergranular space? We consider the shear flow to be a prime candidate. This view is supported by our earlier analyses of different observations (cf. Nesis et al. 1992; Nesis et al. 1996b). In the present work regular as well as exploding granules reveal at their borders also strong velocity gradients (see Fig. 3): On average the line of sight velocity drops from 700 m sec^{-1} to -700 m sec^{-1} over ≈ 600 km; i.e. 300 m sec^{-1} over a pressure scale height (≈ 130 km). The spatial resolution is ≤ 250 km (0.3 arcsec). We expect that such gradients create shear flows at the borders of large granules, which in turn generate turbulence, pressure waves, or thermal spots, as is well known in a general hydrodynamical context (e.g. Tritton 1988). We assert, therefore, that the observed turbulent fluctuations at the granular layers are actually produced locally at the borders of large granules, the place of the shear flows. According to Frisch (1995) the turbulence due to shear flows is not fully developed and thus does not need to follow the Kolmogorov power-law $k^{-5/3}$. This would explain also why the spectral energy density of the measured turbulent fluctuations is characterized by a power-law that differs from the Kolmogorov one (see Nesis et al. 1996a). The findings of Rimmele et al. (1995) and Espagnet et al. (1996) that the sources of pressure waves in the photospheric layers lie in the intergranular space, especially near granules, bear up even more the importance of the shear layers. Moreover, according to Espagnet et al. (1995) shear flow between up- and downflow appears to be the origin for some bright features ("bright sinking plumes"), which they found in the upper and middle photosphere.

We find in the intergranular space of both types of granules a maximum turbulent velocity of 1.5 km s^{-1} in the deepest photosphere (40 km; cf. Fig. 3, panel *a*), which drops down to 0.4 km s^{-1} in the higher layers (200 km; cf. Fig. 3, panel *e*). This is in agreement with a turbulent velocity component of about 1.4 km sec^{-1} predicted by the nonlocal convection model of the solar convection zone by Xiong & Chen (1992).

Beckers & Canfield (1975) dealt with the unresolved velocity (microvelocity) field ξ^2_μ of the photosphere and chromosphere, which they related to line broadening but not explicitly to turbulence. The variation with height of the vertical component of ξ^2_μ can be seen in their Table 2. They found ξ^2_μ = 1.9 km s^{-1} at $\tau_{5000} = 1$ and $\xi^2_\mu = 0.9$ km s^{-1} at 200 km. These values of ξ^2_μ are roughly consistent with our values.

The response of the convectively stable photospheric layers to the dynamical impact of the underlying convectively unstable granulation layers is addressed by our coherence analysis. In the paradigm of a one-dimensional single-input/single-output transfer system (see Fig. 2) the input of the system is the velocity field of the granulation layers–convective as well as turbulent–, while the output represents the velocity field modified by the convectively stable photospheric layers. The layers between input and output are the transfer system $H(k)$.

The results of our coherence analysis show a clearly different correlation behavior of the *small* (≤ 1.5 arcsec) and *large scale* (≥ 1.5 arcsec) structures of the convective velocity field as well as the turbulent velocity field (see Figs. 4 and 6, left column).

– The *small scale turbulent* velocity structures of the granular layers are not correlated with turbulent structures of the higher photospheric layers. The *large scale* structures of the turbulent velocity field are, however, highly correlated (see Fig. 4).

– The *small scale turbulent* velocity structures at 100 km above $\tau_{5000} = 1$ are correlated with similar structures of the overlying layers (see Fig. 5).
– The *small scale convective* velocity structures of the granular layers are not related to similar velocity structures of the higher photospheric layers, although the *large scale* structures of the velocity field are highly correlated (see Fig. 6).
– The *small scale convective* velocity structures at 100 km above $\tau_{5000} = 1$ show a marginal correlation with similar structures of the overlying layers (see Fig. 7).

The high coherence of the large granular velocity scales ($\gtrsim$ 1000 km) in the photosphere up to 200 km above $\tau_{5000} = 1$ (cf. Fig. 6) reflects, from a statistical point of view, the same behavior as found with single regular and exploding granules (cf. Fig. 3). The change in coherence from high values in the large scales range to its practical disappearance in the small scales range could be indicative of different origins of the small scale velocity patterns at the various heights in the photosphere. This holds for the convective as well as for the turbulent velocity patterns. The significant correlation of the small turbulent structures ($\leq$ 1.5 arcsec) in the *upper* overshoot region and the layers above (see Fig. 5, left column) supports the idea of a different origin of the velocity structures at the various photospheric heights and infers the particularity of these layers with respect to those of the first 100 km above $\tau_{5000} = 1$.

The marginal presence of a correlation of the small convective structures, with scales up to $\approx$ 1.2 arcsec, and the lack of any correlation between structures with scales $\leq$ 1.2 arcsec (see Fig. 7, left column) confirms our previous results (Nesis et al. 1993) as well as the results of Espagnet et al. (1995) and reinforces the special properties of the overshoot layers and the layers above with respect to the granulation layers. To explain this difference Nesis & Mattig (1989) and Komm et al. (1990) assumed the existence of secondary motions in these layers induced by the convective motions of the deeper overshoot layers.

In their paper Espagnet et al. (1995) investigate the penetration of the solar granulation into the photosphere by means of a coherence analysis of the data before and after removing the 5-minute oscillations. They argue that the quality of the filtering of the data from 5-min oscillations is important, because these oscillations disturb the computed coherence and phase. As we also mentioned in earlier papers (e.g. Nesis & Mattig 1989), the removal of the 5-minute oscillations from the data has to be done by calculating the $k - \Omega$ diagram if series of spectrograms are available.

Since, however, the ultimate goal of the current paper is the investigation of the behavior of the smallest accessible spatial structures, we decided to select the very best spectrogram of the series and not to contaminate the high detail in this best spectrogram by averaging all spectra or by using the inferior images to filter out oscillations with $k - \Omega$ diagrams (see also the discussion in Nesis et al. 1996). Furthermore, since the interaction between granular motions and 5-min oscillations is most likely a linear process, we expect oscillations to change only the *value* of the coherence, whereas the *form* of the coherence function should be unchanged. It is worthwhile to point out the excellent coincidence between our coherence and phase diagram of the Doppler velocity (Fig. 6) and the corresponding coherence and phase diagram of the filtered velocity shown in Espagnet et al. 1995 (Fig. 7a). This coincidence is remarkable in that it implies a minor influence of the oscillations on those properties of convective motions that are of interest to this paper; we think that one explanation could be the small amplitude of the oscillations in the deep photospheric layers.

5. Conclusion

Our data show that the response of the overshoot region to velocity fluctuations of the deep photosphere depends critically on the size of the structures. The *convective* velocity of large granules ($\geq$ 1000 km) penetrates into the convectively stable overshoot zone up to at least 200 km. This is not the case for small scale velocity patterns, which change more rapidly with height, even though we found indications of marginal coherence in small scales in layers higher than one pressure scale height above $\tau_{5000} = 1$. These indications infer some kind of "dynamical" stratification of the deep photosphere. The *turbulent* velocity field exhibits the same behavior. Our coherence analysis shows that the small scale turbulent field of the granulation layers does not show any correlation with the corresponding field of the overlying layers. However, at 100 km above $\tau_{5000} = 1$ there is a small scale turbulent field of small coherence length, demonstrating again the particularity of the layers one pressure scale height higher than the granulation.

The fact that the exploding and regular granule both show a constant convective velocity in the photosphere shows the lack of a significant velocity gradient with height; and implies that the granular flow *overshoots* into the convectively stable layers, somewhat like a laminar water column penetrates into water of different temperature and density. The reduced turbulence within the granules define the granular flow as quasi-laminar compared to the flow in the intergranular space, the location of enhanced turbulence. The observation of granular shear flow associated with enhanced turbulence infers a turbulent shear at the borders of the granules. The symmetry behavior of the turbulence with respect to the granular flow and its change with height in the photosphere could be interpreted as observational manifestation of diffusion in the photospheric layers. Granular shear flows produce a turbulent velocity field at the granulation layer, which then diffuses to higher layers.

Considering now our results in view of laboratory experiments of convective flows (Tritton 1988) the picture which we gain of the granulation flow is that of a jet or a plume impacting in a liquid of different temperature and density. If this picture of the overshooting convective flow is true, then the borders of the granular flow behave like jet or plume boundary layers, which are associated with turbulence, pressure variations, and wave motions. Such a scenario would explain all our findings and emphasize the important role of the overshoot region for the p-mode excitation.

References

Altrock, R.C., Musman, S., 1976, ApJ 203, 533

Beckers J.M., Canfield R.C., 1975, in Motions in the Solar Atmosphere, AFCRL-TR-75-0592, Sacramento Peak Observatory Project 7649

Brown T.M., 1991, ApJ 371, 396

Christensen-Dalsgaard J., 1996, First Gong meeting, Madison (WI), USA

Espagnet O., Muller R., Roudier Th., et al., 1996, A&A 313, 297

Espagnet O., Muller R., Roudier Th., Mein P., Mein N., 1995, A&AS 109, 79

Frisch U., 1995, Turbulence, Cambridge University Press

Ghosh P., Antia H.M., Chitre S.M., 1995 ApJ 451, 851

Heming O., 1989, Flüsse in der Sonnenphotosphäre, Diplomarbeit, Universität Göttingen.

Holweger H., Müller E., 1974, Solar Phys. 39, 19

Komm R., Mattig W., Nesis A., 1990, A&A 230, 340

Magain P., 1986, A&A 163, 135

Nesis A., Mattig W., 1989, A&A 221, 130

Nesis A., Hammer R., Mattig W., 1990, in Wallerstein G. (ed.) 6th Cambridge Workshop on Cool Stars, Stellar Systems, and the Sun, ASP Conf. Ser. Vol. 9, p. 113

Nesis A., Hanslmeier A., Hammer R., et al., 1992, A&A 253, 561

Nesis A., Hanslmeier A., Hammer R., et al., 1993, A&A 279, 599

Nesis A., Hammer R., Hanslmeier A., et al., 1996a, A&A 310, 973

Nesis A., Hammer R., Schleicher H., 1996b, in Pallavicini R., Dupree A.K. (eds.), 9th Cambridge Workshop on Cool Stars, Stellar Systems, and the Sun, ASP Conf. Ser. Vol. 109, p. 143

Rast M.P., 1995, ApJ 443, 863

Rimmele T.R., Goode P.R., Straus L.H., Stebbins R.T., 1995, in Hoekzema J.T., Domingo V., Fleck B., Battrick B. (eds.), 4th SOHO Workshop: Helioseismology, ESA SP-376, Vol 2, p. 326

Straus Th., Bonaccini D., 1997, A&A, in press

Traving G., 1964, ZfA 60, 167

Tritton D.J., 1988, Physical Fluid Dynamics, 2nd ed., Oxford Science Publications

Xiong D.R., Chen Q.L., 1992, A&A 254, 362

This article was processed by the author using Springer-Verlag LaTeX A&A style file *L-AA* version 3.